PHYSICAL REVIEW FLUIDS **2**, 011301(R) (2017)

Effect of stretching-induced changes in hydrodynamic screening on coil-stretch hysteresis of unentangled polymer solutions

Ranganathan Prabhakar,[1,*] Chandi Sasmal,[2] Duc At Nguyen,[2] Tam Sridhar,[2] and J. Ravi Prakash[2]

[1]*Department of Mechanical and Aerospace Engineering, Monash University, Clayton, Victoria 3800, Australia*

[2]*Department of Chemical Engineering, Monash University, Clayton, Victoria 3800, Australia*

(Received 7 September 2016; published 5 January 2017)

Extensional rheometry and Brownian dynamics simulations of flexible polymer solutions confirm predictions based on blob concepts that coil-stretch hysteresis in extensional flows increases with concentration, reaching a maximum at the critical overlap concentration c^* before progressively vanishing in the semidilute regime. These observations demonstrate that chain stretching strengthens intermolecular hydrodynamic screening in dilute solutions, but weakens it in semidilute solutions. Flow can thus strongly modify the concentration dependence of viscoelastic properties of polymer solutions.

DOI: 10.1103/PhysRevFluids.2.011301

The molecular mechanisms underlying the dynamics of flexible polymers in solution have long held the fascination of physicists [1]. Intramolecular hydrodynamic interactions (HI) play a central role in determining mechanical properties of dilute polymer solutions [2]. The progressive emergence of screening of hydrodynamic (or of excluded-volume) interactions with polymer concentration in semidilute polymer solutions remains relatively unexplored in comparison with phenomena such as entanglements or reptation. Most of our current understanding comes from studies under isotropic conditions close to equilibrium [3,4], but how does stretching in strong flows affect screening? The answer to this question is essential to understand how macroscopic properties depend on polymer concentration in semidilute solutions. This is also significant for applications such as turbulent drag reduction [5], inkjet printing [6], and electrospinning [7], where it is necessary to optimize polymer concentration to achieve good performance.

We use the phenomenon of coil-stretch hysteresis in extensional flows to gain insight into screening of HI in strong flows of polymer solutions. Steady state in extensional flow is primarily the result of a balance between internal resistance of polymer molecules to stretching and the frictional drag force exerted on molecules by the flowing solvent. The relative strength of an extensional flow is expressed in terms of the Weissenberg number, $\mathrm{Wi} \equiv \dot{\varepsilon}\,\lambda_0$, where $\dot{\varepsilon}$ is the strain rate of the imposed flow and λ_0 is the time scale of the slowest relaxation mode of a polymer molecule in a quiescent solution. The friction coefficient of an isolated polymer molecule changes as it is stretched because intramolecular HI and the shielding effect it provides weaken with stretching, exposing segments to solvent flow. De Gennes [8], Hinch [9], and Tanner [10] showed that a consequence of such conformation-dependent friction is that, at any Wi within a window $\mathrm{Wi}_{\mathrm{s-c}} < \mathrm{Wi} < \mathrm{Wi}_{\mathrm{c-s}}$ in extensional flows of dilute polymer solutions, there are two stable states for polymer conformations—a coiled state and a stretched state. Here, $\mathrm{Wi}_{\mathrm{c-s}}$ and $\mathrm{Wi}_{\mathrm{s-c}}$ are the critical values for the coil-to-stretch and stretch-to-coil transitions. Outside this window, only a single state is stable. These predictions have been extensively verified in the dilute regime through observations of strong hysteresis in chain conformations in single-molecule simulations [11–13] and experiments on single DNA molecules [11,14–16], and in rheological properties measured with the filament-stretching extensional rheometer (FiSER) [17,18].

How does coil-stretch hysteresis change with polymer concentration, c? We performed uniaxial extensional flow experiments with the FiSER using solutions of high-molecular-weight polystyrene in a solvent consisting of a mixture of oligomeric styrene and dioctylphthalate [17,19,20]. In these

*prabhakar.ranganathan@monash.edu

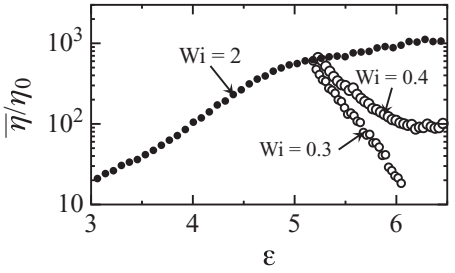

FIG. 1. Transient evolution of $\overline{\eta}$ normalized by the zero-shear rate solution viscosity η_0 to steady state at $\mathrm{Wi} = 2$ (filled circles) and following strain-rate quenches (open circles) to lower values of Wi: the stretch-to-coil transition is identified by noting the quench Wi below which $\overline{\eta}$ relaxes continuously without reaching a steady state within the maximum Hencky strain achievable of about 7.

experiments, polymer solution samples sandwiched between a pair of end plates were stretched by moving the plates rapidly to create slender filaments. The stretching rate was controlled such that a predetermined constant $\dot{\varepsilon}$ was obtained at the necking plane. The polymer contribution to the viscoelastic stress at the neck was calculated from the force measured on the end plate [21,22]. Figure 1 plots the transient evolution of the transient extensional viscosity $\overline{\eta}$ with Hencky strain ε for a typical sample. Two sets of experiments were conducted. In the first, the viscosity was allowed to saturate to give the steady-state viscosity at the Wi corresponding to the strain rate at the neck. The relaxation time λ_0 at each concentration was obtained by small-amplitude oscillatory shear rheometry [20]. In the second set of experiments, after stretching initially at $\mathrm{Wi} = 2\,(>\mathrm{Wi}_{c-s} \approx 1/2)$, the neck strain rate was quenched at a Hencky strain of 5 to a new lower value. Steady-state viscosities were obtained for a range of Wi values. It was possible to detect an abrupt transition Wi_{s-c} below which the polymer stress after quench continually relaxed without reaching a plateau (Fig. 1). Figure 2(a) plots the steady-state polymer contribution to the extensional viscosity $\overline{\eta}_p = \overline{\eta} - 3\eta_s$ (where η_s is the shear viscosity of the Newtonian solvent) against the corresponding Wi at the steady state. A coil-to-stretch transition is observed at $\mathrm{Wi}_{c-s} \sim 1/2$. We find that the size of the coil-stretch hysteresis window does not decrease monotonically with concentration when going from dilute to concentrated solutions. When $c/c^* < 1$, the stretch-to-coil transition at a Wi_{s-c} is first observed to *decrease* with increasing concentration. The hysteresis loop thus widens and only begins to shrink in size when $c > c^*$, where c^* is the concentration at which coils overlap at equilibrium.

We have also observed a similar variation of the hysteresis window in multichain Brownian dynamics (BD) simulations of planar extensional flows of polymer solutions [Fig. 2(b)]. A single polymer molecule in these simulations was represented as a chain of 20 beads connected by finitely-extensible nonlinear elastic (FENE) springs. An optimized Ewald algorithm was used to calculate pairwise HI between beads of all chains in a simulation box. Periodic Kraynik-Reinhelt boundary conditions were used to simulate large strains in planar extensional flows [23]. Excluded volume interactions were neglected. Simulation parameters were chosen to resemble the experimental system. Ensembles with chains initially in their equilibrium configurations and with highly stretched chains were separately simulated to obtain the coiled and stretched-state branches of the hysteresis windows, respectively [20]. From the critical strain rate for the coil-stretch transition, the relaxation time λ_0 was estimated as the value required to obtain $\mathrm{Wi}_{c-s} = 1/2$. It is known that numerical values obtained in bead-spring simulations of extensional flows depend significantly on the number of beads per chain [24,25]. The qualitative similarity with the experimental results, however, suggests that the interesting feature of a maximum in hysteresis at $c/c^* \sim 1$ is likely to remain unchanged even with further resolution of polymer structure at different length scales with larger bead numbers per chain.

The increase in the hysteresis size $\mathrm{Wi}_{c-s}/\mathrm{Wi}_{s-c}$ in the dilute regime before vanishing in semidilute solutions (Fig. 3) is unexpected. The ratio $\mathrm{Wi}_{c-s}/\mathrm{Wi}_{s-c}$ quantifying the size of the hysteresis is known to be proportional to the ratio of ζ_s, the average friction coefficient of a chain stretched close to its

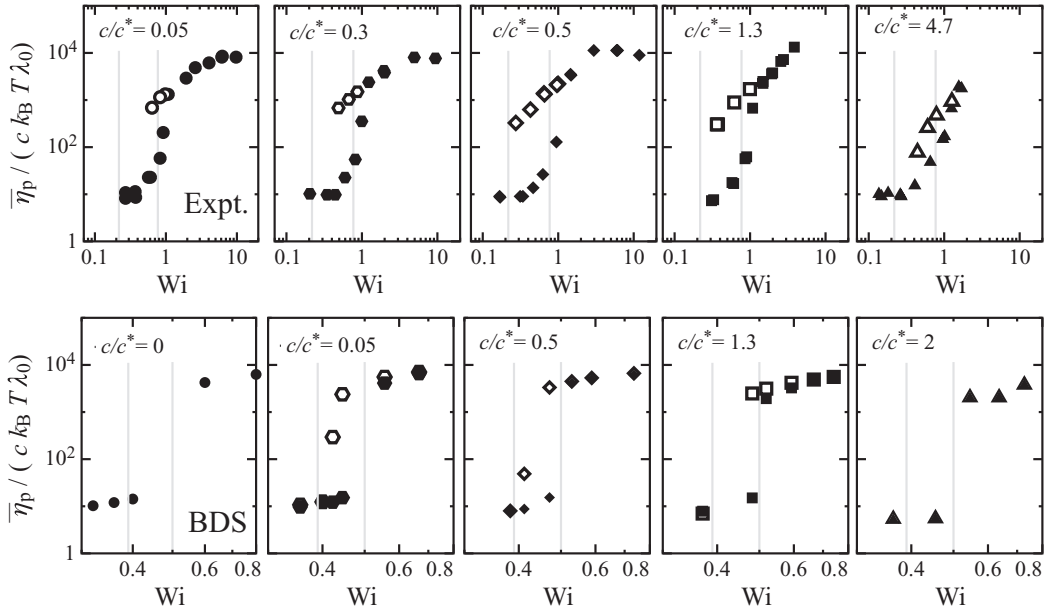

FIG. 2. Concentration dependence of coil-stretch hysteresis in $\overline{\eta}_p$, the polymer contribution to extensional viscosity, in (a) FiSER experiments (top panel) and (b) multichain Brownian dynamics simulations (bottom panel); gray lines indicate the maximum width of the hysteresis windows observed in each case at $c/c^* = 0.5$. Coiled and stretched states are represented by filled and open symbols respectively. Concentration increases from left to right. No hysteresis is observed in the simulations at the lowest and highest concentrations. The number of Kuhn segments $N_K = L^2/R_0^2 \sim 1300$ in both experiments and simulations [20].

contour length L, to ζ_0, the coefficient for an isotropic coil of radius R_0 at equilibrium [8,11,13,15]. Coil-stretch hysteresis can only be observed if ζ_s is significantly larger than ζ_0. In the absence of significant intermolecular interactions, ζ_s is larger than ζ_0 because the shielding due to intramolecular HI of segments in the interior of polymer coils from the solvent velocity field weakens when chains are stretched in flow. In a concentrated solution, on the other hand, where HI is highly screened, chains are expected to be freely draining. The friction coefficient of such Rouse chains is the sum of contributions from every segment irrespective of chain conformation, and $\zeta_0 \sim \zeta_s \sim \eta_s L$: No hysteresis is therefore expected in concentrated solutions.

Prabhakar *et al.* [26] suggested that the maximum in the ratio $\mathrm{Wi}_{c-s}/\mathrm{Wi}_{s-c} \sim \zeta_s/\zeta_0$ is observed because ζ_s and ζ_0 approach the Rouse limit at different rates with increasing concentration. Their

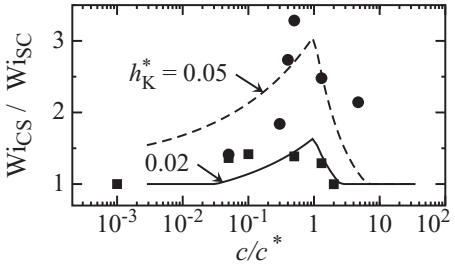

FIG. 3. Concentration dependence of the width of the hysteresis window observed in FiSER experiments (circles) and BD simulations (squares): The continuous and broken curves are predictions of ζ_s/ζ_0 obtained with the blob model for $R = L/2$ and for the hydrodynamic interaction parameters $h_K^* = 0.02$ and 0.05, respectively; all data are for the number of Kuhn segments, $N_K \sim 1300$.

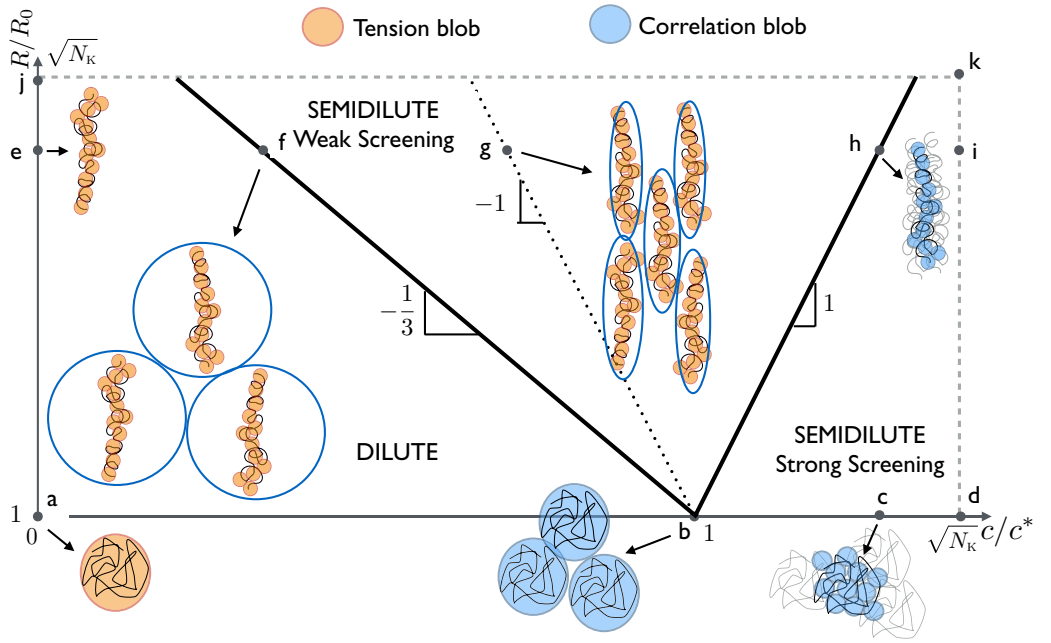

FIG. 4. Stretch–concentration state space for polymer solutions showing the dilute regime and the semidilute regimes with weak and strong hydrodynamic screening. (a) Isolated, equilibrium coils described by Zimm hydrodynamics: Each coil is a single tension blob. (b) Equilibrium coils at critical overlap: Each coil is a single correlation blob. (c) Semidilute coils with correlation blobs smaller than coil size. (d) Concentrated solution with correlation blobs of the same size as a Kuhn segment. (e) Isolated, stretched chains with tension blobs. (f) Chains of tension blobs begin to interact hydrodynamically with a screening length approximately equal to chain length. (g) Critical transverse overlap with anisotropic correlation blobs larger than tension blobs. (h) Transition of stretched chains from weak to strong hydrodynamic screening with correlation and tension blobs of same size. (i) Concentrated solution of stretched chains with correlation blobs of the same size as a Kuhn segment. (j) Fully stretched chains in the dilute limit with tension blobs as small as a single Kuhn segment. (k) Concentrated solution of fully stretched chains.

analysis relating ζ_s and ζ_0 to $c/c\star$ and the polymer stretch ration R/R_0 is based on so-called blob concepts originally proposed by De Gennes [8] and Pincus [27], and is in two parts: the number and size of the two kinds of blobs—correlation and tension blobs—are first related to concentration and stretch, and then ζ_0 and ζ_s are related to these blob characteristics. The salient aspects of that analysis are discussed below with more details in the SI, and the interplay between the two kinds of blobs is summarized in the stretch-concentration state diagram in Fig. 4.

Under quiescent conditions (horizontal axis in Fig. 4), isotropic coils begin to overlap at a critical concentration $c^* \sim R_0^{-3}$. De Gennes [8] argued that in interpenetrating coils, the hydrodynamic screening length ξ_c is given by the scale at which the mean intramolecular segmental density in a typical chain is equal to the mean segmental density of the whole solution [1]. Segments separated by distances larger than ξ_c only experience Rouse-like correlations solely due to backbone connectivity. Beyond critical overlap, each chain can be pictured as a Rouse chain of N_c correlation blobs of size ξ_c.

Analyzing the effect of stretching of isolated chains, Pincus [27] suggested that the competition between random thermal forces and the tension in a chain stretched to a length $R \gg R_0$ brings into play another characteristic length scale, ξ_t. The influence of the applied tension in creating anisotropy in segmental orientation becomes apparent only across scales larger than $\xi_t \sim R_0^2/R$ under θ conditions. Stretched molecules can thus be regarded as chains of N_t tension blobs, each of size ξ_t.

Stretched chains interact hydrodynamically over distances comparable to the polymer stretch R. The boundary between the dilute and semidilute regime is in general given by $R/R_0 \sim (c/c^*)^{-1/3}$. Additionally, in flows where $\mathrm{Wi} \lesssim 1$, conformational fluctuations transverse to the extensional axis can be on the order of R_0 [27]. These can cause stretched chains to overlap even in nominally dilute solutions when $c/c^* \sim (R/R_0)^{-1} \ll 1$. At incipient overlap in stretched chains [e.g., point (g) in Fig. 4], correlation blobs are anisotropic since their size is comparable to that of the whole stretched chain and is hence much larger than a tension blob. With increasing concentration, correlation blobs in stretched chains become smaller and less anisotropic until they become comparable in size to tension blobs [e.g., point (h) in Fig. 4]. Beyond that, correlation blobs are smaller than tension blobs and isotropic, and their size and number do not depend on polymer stretch: Their values are identical to those calculated for equilibrium coils at the same c/c^*.

The argument for relating ζ_0 near equilibrium to c/c^* is well known. The friction coefficient of isotropic coils is nearly constant at the value ζ_Z calculated by Zimm hydrodynamics for coils at infinite dilution until coils begin to overlap at $c/c^* = 1$. At higher concentrations, although HI is screened between blobs, it still persists within each blob. For interpenetrating coils, the Rouse-like average friction of a chain is the sum of the friction coefficients of the correlation blobs, giving $\zeta_0 \sim \zeta_Z\,(c/c^*)$, when $c/c^* > 1$. Scaling analysis suggests that as long as correlation blobs are significantly larger than tension blobs in partially stretched chains, the average friction coefficient of a stretched chain in solution is the same as that of a rodlike blob pole of tension blobs. That is, between points (e) and (h) for chains at a given stretch in Fig. 4, ζ_s is given by slender-body theory for aligned rods of length R and diameter ξ_t [28,29]. In the dilute regime between points (e) and (f), $\zeta_s \sim \eta_s R/\ln(2R/\xi_t)$ is independent of c, whereas between points (f) and (h), ζ_s increases slowly as the logarithm of the volume fraction of tension-blob poles, $\phi_t = cR\xi_t^2$. In this regime, the hydrodynamic screening length is not ξ_c but has the value $\chi \sim \xi_t\,[(1/\phi_t)\ln(1/\phi_t)]^{1/2}]$ estimated for chains treated as poles of tension blobs; $\zeta_s \sim \eta_s R/\ln(2\chi/\xi_t)$ for such blob poles. At concentrations above that of (h), molecules behave as Rouse chains of isotropic correlation blobs of size ξ_c, and $\zeta_s = \zeta_c$ is conformation independent.

Thus, for highly stretched chains between points such as (e) and (h), ζ_s effectively depends logarithmically on concentration over a broad range $(R/R_0)^{-1/3} < c/c^* < R/R_0$. In contrast, between the same concentrations, ζ_0 first remains constant until $c/c^* \sim 1$ and thereafter increases linearly with c/c^*. As a result of this difference in concentration dependence, the ratio ζ_s/ζ_0 first increases weakly until $c/c^* \sim 1$, and then decreases nearly as $(c/c^*)^{-1}$, until $\zeta_s \sim \zeta_0$ at about $c/c^* \sim R/R_0$.

Hence, ζ_s/ζ_0, and consequently, coil-stretch hysteresis, is maximal at $c/c^* \sim 1$. Figure 3 shows good qualitative agreement of the ζ_s/ζ_0 ratio predicted by the scaling model of Prabhakar *et al.* [26], with the hysteresis widths $\mathrm{Wi}_{c-s}/\mathrm{Wi}_{s-c}$ observed in the experiments and simulations. This agreement appears to confirm the existence of a transition from weak to strong hydrodynamic screening in stretched chains. In a nominally dilute solution with $c/c^* \ll 1$, the stronger hydrodynamic interaction between chains when stretched means that macroscopic properties in a dilute solution can exhibit greater sensitivity to concentration in strong flows than at equilibrium; i.e., dilute solutions can self-concentrate [30]. The results presented above imply that unentangled semidilute solutions can conversely self-dilute, with the concentration dependence weakening in strong flows.

An interesting consequence of the behavior above is that significant hysteresis may emerge with increasing concentration in a solution that exhibits little or no hysteresis in the dilute limit. This is observed in our simulation and experimental data (Figs. 2 and 3). The friction coefficient of isolated chains in these systems appears not to change significantly even though chains stretch by more than an order of magnitude in extensional flow. The blob model suggests this may be due to the small values of the hydrodynamic radius of the Kuhn segment in these systems, quantified by the dimensionless parameter h_K^*. This parameter has little influence on the friction of isolated coils: The prefactor to the scaling result $\zeta_Z \sim \eta_s R_0$ has a universal value that is insensitive to h_K^* when N_K is large. In contrast, as the tension blob in a dilute solution shrinks with increasing polymer stretch and becomes comparable in size to a single Kuhn segment, its friction coefficient—and hence the prefactor to the scaling result for ζ_s—is directly proportional to h_K^* [20]. If h_K^* is small enough, the

prefactor can decrease with chain stretching to compensate for the contribution to friction from the change in length. At concentrations comparable to c^*, weak screening can contribute to increase ζ_s sufficiently to cause observable hysteresis. In the strong-screening regime, both ζ_0 and ζ_s increasingly become sensitive to local segmental friction as correlation blobs shrink towards the Kuhn segment with increasing concentration.

Our experiments were performed with uniaxial extensional flows whereas the simulations were in planar extension. This difference plays no significant role for the following reason. The stretched and coiled states that arise in the hysteresis regime effectively represent the two different length scales at which drag forces exerted by the imposed extensional flow balance either the chain tension or thermal forces. The latter determines the size of the chain in the direction transverse to the extensional axis. Since $\mathrm{Wi} \lesssim 1$ in the hysteresis regime, the length scale at which this balance occurs is comparable to the equilibrium coil size [26]. Therefore, transverse chain dimensions in stretched conformations in the hysteresis regime are qualitatively similar in planar and uniaxial flows. At steady states at Wi above the coil-stretch transition, chains are so tautly stretched that it should make little difference to rheooptical properties whether the flow is planar or extensional. This is supported by recent experimental evidence comparing extensional viscosity measurements of entangled solutions in planar and uniaxial extensional flows [31].

The observations reported here have implications for understanding viscoelastic behavior of polymer solutions well beyond the somewhat esoteric phenomenon of coil-stretch hysteresis. Intermolecular interactions are ignored in classical constitutive models used for modeling of viscoelastic flows of nominally dilute solutions. The assumption is that dilute solutions stay dilute. Any polymer solution with a concentration such that $cL^3 > 1$ can be expected to experience significant intermolecular interaction. Analytical arguments suggest that in general the contribution of the dissolved polymer to macroscopic stresses becomes significant just when intermolecular hydrodynamic interactions become important [26,32]. Therefore, fully predicting the influence of polymer concentration in applications may require constitutive models that explicitly account for intermolecular hydrodynamic interactions. The blob model for average chain friction can be used to construct a microstructural constitutive model for viscoelastic stresses in unentangled solutions. Such a model has been demonstrated recently [26] to predict the complex concentration dependence of the dynamics of capillary thinning of liquid bridges [30]. Another question where such a model may be useful concerns the concentration at which polymer-induced turbulent drag reduction sets in. It has been shown that the dynamical slowdown associated with coil-stretch hysteresis can significantly influence chain dynamics in turbulent flows [33,34]. The nontrivial effect of polymer stretching that we have demonstrated here underlines the need for a more detailed examination of hydrodynamic screening in stretched chains. Multichain simulations can be used to test the prediction from blob arguments that transverse chain overlaps do not contribute strongly to screening until correlation blobs become smaller than tension blobs. The insights from such studies could help refine blob-based constitutive models for unentangled polymer solutions.

This work was supported by a monetary grant (DP120101322) from the Australian Research Council and by CPU-time grants from the National Computational Infrastructure, Australia, and eResearch Centre, Monash University.

[1] M. Rubinstein and R. H. Colby, *Polymer Physics* (Oxford University Press, London, UK, 2003).

[2] B. H. Zimm, Dynamics of polymer molecules in dilute solution: Viscoelasticity, flow birefringence, and dielectric loss, J. Chem. Phys. **24**, 269 (1956).

[3] P. Ahlrichs, R. Everaers, and B. Dünweg, Screening of hydrodynamic interactions in semidilute polymer solutions: A computer simulation study, Phys. Rev. E **64**, 040501 (2001).

[4] A. Jain, B. Dünweg, and J. Prakash, Dynamic Crossover Scaling in Polymer Solutions, Phys. Rev. Lett. **109**, 088302 (2012).

[5] C. M. White and M. G. Mungal, Mechanics and prediction of turbulent drag reduction with polymer additives, Annu. Rev. Fluid Mech. **40**, 235 (2008).
[6] H. Sirringhaus, T. Kawase, R. H. Friend, T. Shimoda, M. Inbasekaran, W. Wu, and E. P. Woo, High-resolution inkjet printing of all-polymer transistor circuits, Science **290**, 2123 (2000).
[7] C. Wang, C.-H. Hsu, and J.-H. Lin, Scaling laws in electrospinning of polystyrene solutions, Macromol. **39**, 7662 (2006).
[8] P.-G. De Gennes, Coil-stretch transition of dilute flexible polymers under ultrahigh velocity-gradients, J. Chem. Phys. **60**, 5030 (1974).
[9] E. J. Hinch, Mechanical models of dilute polymer-solutions in strong flows, Phys. Fluids **20**, S22 (1977).
[10] R. I. Tanner, Stresses in dilute solutions of bead-nonlinear-spring macromolecules, III: Friction coefficient varying with dumbbell extension, J. Rheol. **19**, 557 (1975).
[11] C. M. Schroeder, E. S. G. Shaqfeh, and S. Chu, Effect of hydrodynamic interactions on DNA dynamics in extensional flow: Simulation and single molecule experiment, Macromol. **37**, 9242 (2004).
[12] R. Prabhakar and J. R. Prakash, Gaussian approximation for finitely extensible bead-spring chains with hydrodynamic interaction, J. Rheol. **50**, 561 (2006).
[13] C.-C. Hsieh and R. G. Larson, Prediction of coil-stretch hysteresis for dilute polystyrene molecules in extensional flow, J. Rheol. **49**, 1081 (2005).
[14] T. T. Perkins, D. E. Smith, and S. Chu, Single polymer dynamics in an elongational flow, Science **276**, 2016 (1997).
[15] C. M. Schroeder, H. P. Babcock, E. S. G. Shaqfeh, and S. Chu, Observation of polymer conformation hysteresis in extensional flow, Science **301**, 1515 (2003).
[16] E. S. G. Shaqfeh, The dynamics of single-molecule DNA in flow, J. Non-Newtonian Fluid Mech. **130**, 1 (2005).
[17] T. Sridhar, D. A. Nguyen, R. Prabhakar, and J. R. Prakash, Rheological Observation of Glassy Dynamics of Dilute Polymer Solutions Near the Coil-Stretch Transition in Elongational Flows, Phys. Rev. Lett. **98**, 167801 (2007).
[18] R. G. Larson, The rheology of dilute solutions of flexible polymers: Progress and problems, J. Rheol. **49**, 1 (2005).
[19] R. K. Gupta, D. A. Nguyen, and T. Sridhar, Extensional viscosity of dilute polystyrene solutions: Effect of concentration and molecular weight, Phys. Fluids **12**, 1296 (2000).
[20] See Supplemental Material at http://link.aps.org/supplemental/10.1103/PhysRevFluids.2.011301 for more information on experimental materials and methods, Brownian Dynamics algorithm and simulations, and blob theory for friction in partially stretched polymer chains.
[21] V. Tirtaatmadja and T. Sridhar, A filament stretching device for measurement of extensional viscosity, J. Rheol. **37**, 1081 (1993).
[22] G. H. McKinley and T. Sridhar, Filament-stretching rheometry of complex fluids, Annu. Rev. Fluid Mech. **34**, 375 (2002).
[23] A. Jain, C. Sasmal, R. Hartcamp, B. D. Todd, and J. R. Prakash, Brownian dynamics simulations of planar mixed flows of polymer solutions at finite concentrations, Chem. Eng. Sci. **121**, 245 (2015).
[24] R. Prabhakar, J. R. Prakash, and T. Sridhar, A successive fine-graining scheme for predicting the rheological properties of dilute polymer solutions, J. Rheol. **48**, 1251 (2004).
[25] P. Sunthar, D. A. Nguyen, R. Dubbelboer, J. R. Prakash, and T. Sridhar, Measurement and prediction of the elongational stress growth in a dilute solution of DNA molecules, Macromol. **38**, 10200 (2005).
[26] R. Prabhakar, S. Gadkari, T. Gopesh, and M. J. Shaw, Influence of stretching induced self-concentration and self-dilution on coil-stretch hysteresis and capillary thinning of unentangled polymer solutions, J. Rheol. **60**, 345 (2016).
[27] P. Pincus, Excluded volume effects and stretched polymer chains, Macromol. **9**, 386 (1976).
[28] G. K. Batchelor, Slender-body theory for particles of arbitrary cross-section in Stokes flow, J. Fluid. Mech. **44**, 419 (1970).
[29] M. B. Mackaplow and E. S. G. Shaqfeh, A numerical study of the rheological properties of suspensions of rigid, non-Brownian fibres, J. Fluid Mech. **329**, 155 (1996).

[30] C. Clasen, J. P. Plog, W. M. Kulicke, M. Owens, C. Macosko, L. E. Scriven, M. Verani, and G. H. McKinley, How dilute are dilute solutions in extensional flows? J. Rheol. **50**, 849 (2006).

[31] D. A. Nguyen, P. K. Bhattacharjee, and T. Sridhar, Response of an entangled polymer solution to uniaxial and planar deformation, J. Rheol. **59**, 821 (2015).

[32] H. C. Öttinger, *Stochastic Processes in Polymeric Fluids* (Springer-Verlag, Berlin, 1996).

[33] A. Celani, A. Puliafito, and D. Vincenzi, Dynamical Slowdown of Polymers in Laminar and Random Flows, Phys. Rev. Lett. **97**, 118301 (2006).

[34] A. Ahmad and D. Vincenzi, Polymer stretching in the inertial range of turbulence, Phys. Rev. E **93**, 052605 (2016).